Computer Communications 120 (2018) 22–31

Contents lists available at ScienceDirect

Computer Communications

journal homepage: www.elsevier.com/locate/comcom

Scalable video multicast using inter-layered superposition and network-coded cooperation over MIMO relay systems

Phuc Chau[a], Jitae Shin*[,a], Jaehoon (Paul) Jeong[b]

[a] School of Electronic and Electrical Engineering, Sungkyunkwan University, Suwon, South Korea
[b] Department of Interaction Science, Sungkyunkwan University, Suwon, South Korea

ARTICLE INFO

Keywords:
Network coding
Video multicast
Scalable video
Relay-assisted cellular networks

ABSTRACT

The adoption of scalable video coding (SVC) for video multicast services is a promising solution for providing efficient streaming under channel heterogeneity, since SVC can support quality scalability with high coding efficiency. The scalability allows receivers to experience video quality according to their channel conditions. Nevertheless, the scalable video layers are inter-dependent; if a layer of the scalable video is lost, all subsequent layers that depend on the lost layer are downloaded but not rendered, which leads to a low video quality and bandwidth inefficiency. Consequently, unequal error protection among scalable video layers needs to be addressed in a bandwidth-efficient manner. This paper proposes a scalable video multicast scheme over relay-based cellular networks, consisting of two main components: inter-layered superposition in the first phase and digital network coding in the second phase. In this joint design, the proposed inter-layered superposition coding provides incremental service quality according to average channel conditions, as well as unequal error protection under channel heterogeneity. Furthermore, the network-coded cooperation, implemented by mixing all decoded signals at the relay, improves bandwidth efficiency by reducing the number of transmissions in the second phase. The proposed scheme aims to increase the number of users experiencing a maximal number of rendered video layers as well as bandwidth efficiency. We also derive the relevant channel capacities of scalable layers for performance analysis. Numerical results, consisting of a cumulative distribution function of channel capacity, achievable video data rate, and video quality measurement, confirm that our design objective can be achieved for video multicast over multiple-input and multiple-output relay-based cellular networks.

1. Introduction

Scalable video coding (SVC) has been widely used in many applications with heterogeneous clients [1–5] and for multiple-input and multiple-output (MIMO) systems [6–9]. It can support spatial (i.e., resolution), temporal (i.e., frame rate), and amplitude (i.e., quality) scalability [10], which allows the wireless receiver to experience different levels of video quality depending on the received signal strength. The video content is split into multiple scalable video layers (i.e., several subset bitstreams) consisting of a base layer (BL) and multiple enhancement layers (ELs) [11]. The BL bitstream carries the base video content (i.e., typical quality of the video), while the additional ELs contain refinement information for enhancing the perceived visual quality or high resolution. The scalable video layers form an inter-dependent structure because the higher layer depends on the lower layer. Hence, a bitstream layer is only rendered successfully if the lower layer is rendered. The video quality experienced by the receiver depends on the number of rendered video bitstreams. A greater number of rendered layers leads to a higher perceived video quality. However, two challenges need to be considered, in particular, in scalable video transmission. First, the delivery of additional layer bitstreams carried in transmission causes an increase in terms of time or bandwidth [3,4]. Second, if a layer is lost, subsequent layers depending on the lost layer are useless (i.e., not rendered), even though they can be successfully decoded [5–8]. To address these challenges, we need to provide unequal error protection (UEP) for scalable video layers in a resource-efficient manner.

Cisco Visual Networking Index Forecast predicts an increase in mobile data traffic to 49 exabytes per month by 2021 [12]. To meet the fast increment of mobile data traffic growth, 5G ultra-dense cellular networks have been investigated by jointly composing small cells and macrocells [13]. Small base stations (BSs) (i.e., microcells) are distributed within the macrocell's coverage. Both the macrocell and microcell BSs can independently and transparently manage the data traffic demand from associated subscribers. The small cell concept can increase system throughput in two ways:1) the common bandwidth

* Corresponding author.
E-mail addresses: cmphuc@skku.edu (P. Chau), jtshin@skku.edu (J. Shin), pauljeong@skku.edu (J.P. Jeong).

https://doi.org/10.1016/j.comcom.2018.02.016
Received 27 October 2016; Received in revised form 14 January 2018; Accepted 19 February 2018
Available online 22 February 2018
0140-3664/ © 2018 Elsevier B.V. All rights reserved.

resources can be used by different microcells in various regions and 2) users in a microcell's coverage have a higher probability of line-of-sight connection to microcell BSs [14].

Herein, we study the adoption of SVC for a video multicast service over ultra-dense cellular networks with a single gateway, where a BS (i.e., macrocell BS equipped with multiple antennas) transmits multiple SVC layers to a group of users with the assistance of a dedicated relay (i.e., microcell). Our design objective is to improve system performance in terms of an increase in the number of users experiencing full video quality with bandwidth efficiency (i.e., reduction in the number of transmissions leading to an increase in efficient bandwidth utilization). We propose a video multicast method, named ISC-DNC, which uses inter-layered superposition coding (ISC) to transmit all SVC layers sequentially with different time slots in the first phase. The dedicated relay performs digital network coding (DNC) to transmit an additional signal containing all SVC layers in the second phase. The proposed ISC can provide UEP and improve the system performance as scalable layers are transmitted separately in time-shared transmission with reasonable configuration parameters. In addition, DNC along with an efficient estimation algorithm can increase the bandwidth efficiency since the relay only uses one transmission slot in the second phase through the dedicated MIMO relay-based cooperation. Specifically, our contributions are as follows:

- The proposed ISC-DNC scheme can provide UEP among the SVC layers by simply adjusting the importance-dividing factor (IDF) parameters based on the channel states of user equipment (UEs) (details in Section 3.2.1). Even when almost all UEs experience a bad channel state, they can enjoy typical video quality (i.e., at least the BL rendered) since the importance of the BL is adjusted depending on the distribution of channel states among the UEs.
- The number of multiple SVC layers carried in transmission is increased to allow the UEs to be more flexible, so that users can enjoy the corresponding video quality according to the channel state, with L different classes of video quality. In contrast, the recent studies only allow a superposed signal carrying two SVC layers (i.e., a BL and an EL) [6,7].
- The interference caused by superposed signals is traditionally considered harmful. However, our proposed ISC, along with the efficient estimation algorithm (EEA) for network-coded cooperation, can transform this harmfulness into additional system performance gain and better bandwidth efficiency.
- We conducted a formal capacity analysis to assess the effectiveness of our multicast transmission scheme. A numerical simulation was also performed for the assessment of capacity and achievable video data rate. Based on these analyses, we show that the proposed scheme satisfactorily matches our design objective. Furthermore, video quality measurement was conducted in terms of peak signal-to-noise ratio (PSNR) as a quality metric for comparison with other prevalent schemes.

The remainder of this paper is organized as follows. We describe related work and the system model and our proposed video multicast method in Section 2 and Section 3.2, respectively. In Section 4, we formulate the channel capacity analysis of scalable layers. Furthermore, we derive system performance in terms of achievable video bitrates and video quality measurements and compare our scheme with other schemes in Section 5. Finally, we conclude our paper and present future work in Section 6.

2. Related work

The greatest challenge in multicast systems is channel heterogeneity, whereby the channel states of the UE vary over time. If we define quality of service (QoS) with respect to the user receiving the lowest signal-to-noise ratio (SNR) (i.e., guaranteeing that all users with a better channel condition can achieve at least the defined QoS), it leads to a bottleneck issue since other users who experience better channel conditions must experience the lowest QoS [15]. Thus, such users are provided with the lowest video quality. This bottleneck issue can be solved by cooperative communication. In the literature, cooperative communication consists of two phases: a BS broadcasts the content to the receiver and relay in the first phase, and then, a relay station (RS) relays the received signal (probably using amplify-and-forward (AF) and decode-and-forward (DF)) to the receiver in the second phase. The receiver uses two signals from the BS and RS for decoding. Hence, users experiencing bad channel conditions in the first phase still have a chance to receive information from the relay in the second phase.

To utilize the advantage of cooperative communication, many studies have investigated SVC multicast applications over relay-based networks with the assistance of users [6] or a dedicated relay [7]. The simplest method to create UEP among SVC layers is to use different channels to deliver the SVC layers. The better channel delivers the layer with higher importance. However, this method causes inefficient bandwidth utilization since the use of additional channels increases. Chih-Hung et al. [6] proposed cooperative wireless broadcast for scalable video delivery (CWB-SVC) to tackle the two aforementioned problems of a scalable video (i.e., additional resource burden and UEP). They assumed that the SVC bitstream is partitioned into two-layer bitstreams consisting of a BL and an EL, where the BL is encoded using space-time block coding (STBC) and the additional EL is superposed with the BL into a signal and assigned varying degrees of importance. Instead of using different channels for two SVC layers, the BS broadcasts the superposed signal consisting of the BL and EL to users in the first phase (i.e., BL and EL signals are superposed into a single signal for transmission). Then, the users experiencing good channel conditions help those experiencing bad channel conditions by delivering the decoded BL signal in the second phase. The authors showed that the use of the superposition coding technique can mitigate the issue of additional burden on transmission resources (i.e., time or bandwidth) for multiple video streams, since the BS only uses one superposed signal to carry two SVC layers (i.e., BL and EL are superposed into one signal). Moreover, UEP can be provided by controlling the power-dividing factor (i.e., a parameter can be used for controlling the importance among SVC layers) of the superposed signal. Hwang et al. [7] used the same approach, but employed dedicated relay-based delivery as well as the superposition of beamforming (i.e., conveying BL) and STBC (i.e., conveying EL) for the transmission of an eNB as a BS. Their scheme is called CMS-SVC. There are two main benefits of using dedicated relay-based delivery, compared to user relay-based delivery. First, the channel medium between the eNB and dedicated relay is line of sight, leading to stable and high data-rate transmission. This means that the information transmitted from the dedicated relay supports high reliability. Second, the dedicated relay provides better transmission range without any burden of synchronization issue among users. In [7], users close to the relay had more chance to receive all transmitted scalable layers. This leads to an increase in system performance in terms of the number of users successfully decoding the BL. This dedicated relay does not require any additional transmission for the EL since the relay only broadcasts a decoded BL signal. Recently, Feng et al. [16] studied the problem of joint downlink and device-to-device (D2D) transmissions for SVC streaming using network coded cooperation. Authors formulated the problem into a mixed integer non-linear programming problem to increase the performance as the number of users in multicast group increases. Douik et al. [17] reviewed instantly decodable network coding schemes from centralized to D2D communications. Authors showed that users exchange network coded packets from different users can speed up the recovery capability of the missing packets. Karim et al. [18] proposed rate-aware approach using instantly decodable network coding for video distortion reduction. Authors proposed heuristic algorithm to reduce the video distortion before the deadline and increase the perceptual video quality to individual users

regardless of their channel conditions.

All the aforementioned studies satisfactorily address UEP using the scalability of SVC and ensure bandwidth efficiency in terms of non-incremental transmission time (i.e., eNB does not need to use additional transmission time slots to deliver the additional SVC layers). However, system performance should be enhanced in terms of growth in the number of users enjoying full video quality rather than only base video quality (i.e., only BL is rendered), where only the BL is guaranteed to be successfully decoded. Kim et al. [19] exploited a time-shared transmission to deliver multiple SVC layers, where an individual time slot is used to deliver each layer. They proposed an optimal layered resource allocation algorithm for video broadcast in order to improve the quality of video services for users experiencing varying channel conditions. Since all layers are transmitted separately with reasonable consideration of resource allocation, the proposed scheme can increase the number of users experiencing the complete video bitstream. However, this time-shared transmission mechanism leads to an increase in transmission time. Recently, Fuente et al. [20] proposed radio resource management (RRM) strategies which consider the spectral efficiency and fairness among users. The proposed RRM strategy is based on multicast subgrouping to reduce searching space and to optimize aggregated data rate. Huang et al. [21] proposed a multi-generation packet scheduling problem using dynamic programming algorithm to maximize the number of users experiencing good video quality. The proposed scheme selects the optimal SVC layer and a suitable number of redundant packets in the transmission pipeline.

Therefore, the trade-off between the burden of additional transmission resources for multiple video layers and system performance needs to be investigated carefully. Ahlswede et al. [22] proposed network coding (NC) to provide bandwidth efficiency in terms of reduction in the number of transmissions by applying a linear combination of several packets into a coded packet for transmission. The use of NC at the relay was proposed to achieve significant bandwidth efficiency in terms of reduction in the additional number of transmissions. The relay only uses one more transmission slot in the second phase instead of multiple transmissions corresponding to the number of source nodes (i.e., the nodes sending data toward relay) [23]. There are two types of NC at the physical layer: analog network coding (ANC) and DNC. In ANC, the relay simply combines the incoming signals without decoding the received signals. On the contrary, in DNC, the relay decodes incoming signals and combines all decoded signals into one transmission. Thus, for interference reduction and avoidance of the power allocation issue, DNC is preferred. Many studies [24,25] have been conducted on NC to improve system performance by reducing the number of transmissions.

3. Proposed video multicast scheme

3.1. System model

Fig. 1 depicts a cellular network with a dedicated RS. Assume that a group of users N are distributed uniformly in the RS's coverage. Let d_{RS,UE_n} be the distance between the RS and UE_n. A probability density function of the distance d_{RS,UE_n} from the RS is expressed as follows:

$$f_{\mathbf{d}}(d_{RS,UE_n}) = \frac{2d_{RS,UE_n}}{d_{RS}^2}, \qquad 0 < d_{RS,UE_n} < d_{RS}, \tag{1}$$

where d_{RS} is the radius of the RS's coverage. The eNB broadcasts scalable video bitstreams toward a group of UEs within the RS's cell coverage; the RS then helps the UE within its coverage area to enhance perceptual video quality, as well as bandwidth efficiency, at the UE.

Multiple-antenna transmission techniques are employed with the assumption that the eNB, RS, and UEs are equipped with multiple antennas. Let M_b,M_r, and M_u be the number of antennas at the eNB, RS, and UE, respectively. $\mathbf{H}_{r,i}$ and $\mathbf{H}_{n,i}$ are channel matrices from the eNB

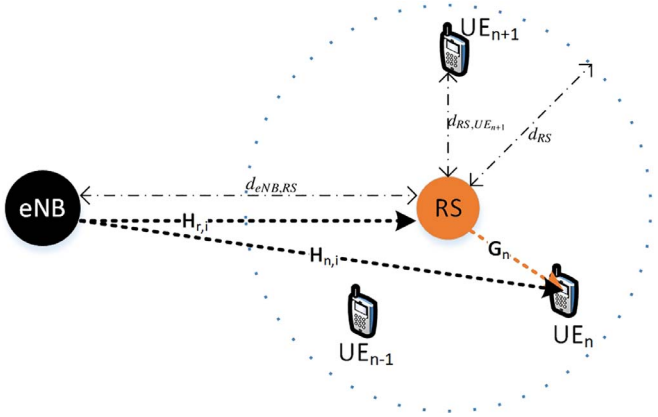

Fig. 1. Dedicated relay-based cellular network.

toward the RS and UE_n at time slot i with dimensions $M_r \times M_b$ and $M_u \times M_b$, respectively. Let $\mathbf{G}_n$ be the channel matrix from the RS toward UE_n with dimensions $M_u \times M_r$. The elements of channel matrices are assumed to be independent and identically distributed (i.i.d.) Rayleigh fading channels, where the channel coefficient remains unchanged during symbol transmission. Let $P_{b,\ i}$ and P_r be the eNB power at time slot i and the RS power, respectively.

The video is encoded into multiple-layered video bitstreams composed of a BL and $L-1$ additional ELs using scalable video codec. Let V_l be the target video bitrate of the l^{th} SVC layer. The video bitrate is the number of bits that are processed in a unit of time. Generally, a higher video bitrate can provide higher image quality in the video output. Suppose that each UE sends the feedback channel quality indicator (CQI) signal to the eNB at the beginning of transmission duration. The CQI report is used to measure the radio channel quality [26]. We classify the channel conditions into three states: bad, fair, and good [27]–based on the mean received SNR values from all UEs (i.e., SNR_{mean}):

- Bad: $\text{SNR}_{mean} \leq Th_{fair}$, as many UEs experience deep fading, where Th_{fair} is the threshold of a fair channel state.
- Fair: $Th_{fair} < \text{SNR}_{mean} \leq Th_{good}$, as the number of UEs experiencing deep fading is equal to that of UEs experiencing satisfactory channel states, where Th_{good} is the threshold of a good channel state.
- Good: $Th_{good} < \text{SNR}_{mean}$, as most UEs experience satisfactory channel states.

3.2. Proposed ISC-DNC scheme

This paper proposes a multicast transmission scheme for scalable video associated with specific scalable characteristics (i.e., UEP and the issue of additional resource burden to time and bandwidth) based on channel condition information. The system is assumed to be synchronous between eNB and RS, and operates in the half-duplex mode, where the transmissions of the first and second phases are predefined in different time slots. The proposed ISC-DNC scheme is presented as follows:

(i) eNB evaluates the multicast criterion CQI from all UEs to determine the mean value of the received SNR values based on the collected CQIs.
(ii) The importance of each SVC layer is determined (detailed explanation in Section 3.2.1): the output IDF is used to create UEP among the SVC layers corresponding to the information of target video bitrates and channel states. The selection of IDF aims to enhance the video quality with UEP as the number of UEs experiencing the bad channel state increases.
(iii) The complete transmission consists of two phases: the eNB performs the proposed ISC (explained in Section 3.2.1) with the

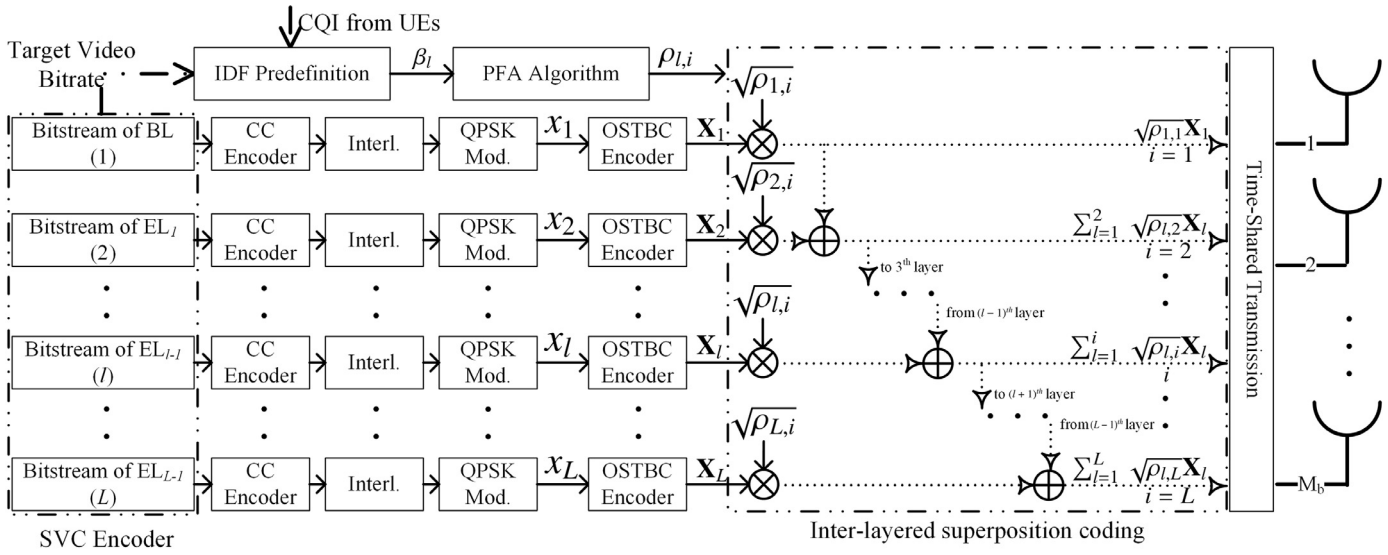

Fig. 2. eNB's architecture with the proposed ISC.

predefined IDF and broadcasts L multiple-layered video bitstreams sequentially in time-shared transmission in the first phase. Thereafter, the RS performs DNC with the assistance of the proposed EEA and transmits a network-coded signal toward the UEs in the following time slot in the second phase (detailed explanation in Section 3.2.2).

(iv) Decoding at UE using signals from eNB and RS (explained in Section 3.2.3): UE performs the proposed EEA using signals from the eNB in the first phase to transform harmful interference into useful estimates of received signals. Then, the UE uses a signal from the RS and performs the proposed iterative decoding algorithm (IDA) with the output estimates of the EEA to decode the received signals from both the eNB and RS (i.e., L signals from eNB and 1 signal from RS).

3.2.1. ISC at eNB

Fig. 2 represents the architectures of the sender (i.e., eNB). In the first phase at the eNB, SVC bitstreams are transmitted in L time slots. L-layered video bitstreams are sequentially sent to channel coding (CC) encoders and interleaving (Interl.) blocks for both error correction in transmission and significant increase in coding gain. The outputs are mapped into QPSK-modulated symbols x_l with $l \in [1: L]$. We propose ISC to create the UEP and implement scalability for scalable layers with the given rate distortion information obtained from the video encoder. Without loss of generality, we assume that the symbol length from the modulation block has the same length (i.e., using the same modulation) since our proposed scheme focuses on the benefit of superposition coding and network-coded cooperation.

The output signal $\mathbf{X}_l$ of the orthogonal spacetime block-coded (OSTBC) encoder is a signal matrix of the l^{th} SVC layer used for transmission by M_b antennas at the eNB for the duration of T_1 symbols is the $M_b \times T_1$ OSTBC signal. This technique is highly attractive for use in practical applications due to its low decoding complexity and highly reliable transmission [28]. The signal matrix $\mathbf{X}_l$ with $M_b = 4$, $T_1 = 4$, and a spatial code rate of $\frac{3}{4}$ can be represented as follows:

$$\mathbf{X}_l = \begin{bmatrix} x_{l,1} & -x_{l,2}^* & x_{l,3}^* & 0 \\ x_{l,2} & x_{l,1}^* & 0 & x_{l,3}^* \\ x_{l,3} & 0 & -x_{l,1}^* & -x_{l,2}^* \\ 0 & x_{l,3} & x_{l,2} & -x_{l,1} \end{bmatrix}, \tag{2}$$

where $x_{l,a}$ is a symbol element in OSTBC at the l^{th} SVC layer of the a^{th} antenna ($a \le M_b$ depending on the spatial code rate, $a = 1, 2, 3$ in this case) and $(\cdot)^*$ denotes the Hermitian transpose.

In the conventional time-shared transmission, the eNB sequentially broadcasts L OSTBC signals starting from the BL. To create a UEP for SVC, we propose the ISC, in which the l^{th} transmitted signal is the superposition of all lower $l-1$ OSTBC signals (Fig. 2). For instance, the BL signal is carried in all L transmitted OSTBC signals, EL$_1$ appears when using $L-1$ signals, and the least important layer L is only carried in the last OSTBC signal. Hence, the BL gets maximum error protection since it is carried in all transmitted signals (i.e., if a signal is lost, we can use other signals to decode the BL with high probability). The higher SVC layer gets lower protection.

The received signals of the i^{th} slot at the RS and UE$_n$ are as follows:

$$\begin{aligned} \mathbf{R}_{r,i}^{(1)} &= \mathbf{H}_{r,i} \sum_{l=1}^{i} \sqrt{\rho_{l,i}}\mathbf{X}_l + \mathbf{N}_{r,i}^{(1)}, \\ \mathbf{R}_{n,i}^{(1)} &= \mathbf{H}_{n,i} \sum_{l=1}^{i} \sqrt{\rho_{l,i}}\mathbf{X}_l + \mathbf{N}_{n,i}^{(1)}, \end{aligned} \tag{3}$$

where $i = [1: L]$ is the transmission slot index, $\mathbf{N}_{r,i}^{(1)}$ and $\mathbf{N}_{n,i}^{(1)}$ are $\mathcal{CN}(0, 1)$-distributed white noise matrices at the RS and UE$_n$ with dimensions $M_r \times T_1$ and $M_u \times T_1$ in the first phase (i.e., superscript (1)), respectively, and $\rho_{l,i}$ is a power-dividing factor of the l^{th} SVC layer signal in the i^{th} superposed signal with $\sum_{l=1}^{i} \rho_{l,i} = 1$. We can say that $\rho_{l,i}$ is the power-dividing factor of the l^{th} SVC layer signal in the i^{th} transmission slot. The following upper-triangular L by L matrix represents the power-dividing factors during a total of L time slots.

$$\begin{bmatrix} \rho_{1,1} & \rho_{1,2} & \rho_{1,3} & \cdots & \rho_{1,L} \\ 0 & \rho_{2,2} & \rho_{2,3} & \cdots & \rho_{2,L} \\ 0 & 0 & \rho_{3,3} & \cdots & \rho_{3,L} \\ \cdots & \cdots & \cdots & \cdots & \cdots \\ 0 & 0 & 0 & \cdots & \rho_{L,L} \end{bmatrix}.$$

Note that the inputs of ISC are the information of the target video bitrate V_l of each l^{th} SVC layer from the SVC encoder and CQI from UEs. Let β_l be the IDF of the l^{th} SVC layer, the choice of β_l flexibly provides the control ability of UEP among scalable layers according to the target video bitrates from the video encoder (Fig. 2) and the channel condition. Upon predefining the IDF set, we use Algorithm 1 to convert β_l to each power-dividing factor $\rho_{l,i}$ of the l^{th} SVC layer signal in the i^{th} transmission slot. The conversion from β_l to $\rho_{l,i}$ is based on the following definition:

$$\beta_l = \frac{\sum_{i=l}^{L} \rho_{l,i}}{L}. \tag{4}$$

Input: Predefined IDF set
Output: The matrix of power-dividing factor initialization
$\rho_{l,i} = 0, \forall\, 1 \le l \le L, 1 \le i \le L$

1: **procedure**
2: **for** i = 1 to L **do**
3: **if** $\beta_i \ge \beta_{mean}$ **then** // with $\beta_{mean} = \sum_{i=1}^{L} \beta_i / L$
4: $\rho_{i,i} = 1$
5: **else**
6: $\rho_{i,i} = \beta_i / \beta_{mean}$
7: **for** l = i-1 to 1 **do**
8: **if** $\beta_l > \beta_{mean}$ **then**
9: $\rho_{l,i} = 1 - \sum_{l}^{L} \rho_{l,i}$

Algorithm 1. Power-dividing factor allocation (PFA) Algorithm.

The assignment of the IDF set is presented as follows:

- Under a good channel condition (i.e., $Th_{good} < \text{SNR}_{mean}$): when most of UEs experience a good channel condition, we target all users achieving the target video bitrate of all SVC layers. Hence, the value of IDF of the l^{th} SVC layer is simply determined as follows:

$$\beta_l = \frac{V_l}{\sum_{l=1}^{L} V_l}. \tag{5}$$

- Under a fair channel condition (i.e., $Th_{fair} < \text{SNR}_{mean} \le Th_{good}$): most UEs experience a fair channel state and there are some UEs experiencing bad or good channel states. Our design objective aims to increase the number of UEs that can enjoy the typical video quality as well as bandwidth efficiency. In this case, if we keep transmitting the SVC bitstreams with the above predefined IDF, power utilization will be inefficient since most UEs cannot decode all L SVC layers (i.e., the power allocation for L^{th} is unnecessary). To increase the efficient power utilization, we subtract the power of the last enhancement SVC layer EL_L in order to assign more power to the BL. The IDFs of BL and EL_L are defined as follows:

$$\begin{aligned}\beta_1 &= \frac{V_1}{\sum_{l=1}^{L} V_l} + \left(1 - \frac{\sum_{n=1}^{N} \mathbf{I}(SNR_n > Th_{good})}{N}\right)\frac{V_L}{\sum_{l=1}^{L} V_l},\\ \beta_L &= \frac{\sum_{n=1}^{N} \mathbf{I}(SNR_n > Th_{good})}{N}\frac{V_L}{\sum_{l=1}^{L} V_l},\end{aligned} \tag{6}$$

where $\mathbf{I}(\cdot)$ is an indicator function that returns 1 when the condition is true; otherwise, 0. We partition the IDF of EL_L by the ratio of the number of UEs experiencing good channel state and the total number of UEs (i.e., N). The values of β_2 to β_{L-1} are defined using Eq. (5).

- Under a bad channel condition (i.e., $\text{SNR}_{mean} \le Th_{fair}$): since most of UEs experience a bad channel state, power allocation for BL needs to be increased. We share the power of two ELs (i.e., EL_{L-1} and EL_L) to enhance the power allocation of the BL. The values of β_2 to β_{L-2} are determined using Eq. (5). The IDFs of BL, EL_{L-1}, and EL_L are re-defined as follows:

$$\begin{aligned}\beta_1 &= \frac{V_1}{\sum_{l=1}^{L} V_l} + \left(1 - \frac{\sum_{n=1}^{N} \mathbf{I}(Th_{fair} < SNR_n \le Th_{good})}{N}\right)\frac{V_{L-1}}{\sum_{l=1}^{L} V_l}\\ &\quad + \left(1 - \frac{\sum_{n=1}^{N} \mathbf{I}(SNR_n > Th_{good})}{N}\right)\frac{V_L}{\sum_{l=1}^{L} V_l},\\ \beta_{L-1} &= \frac{\sum_{n=1}^{N} \mathbf{I}(Th_{fair} < SNR_n \le Th_{good})}{N}\frac{V_{L-1}}{\sum_{l=1}^{L} V_l}\\ \beta_L &= \frac{\sum_{n=1}^{N} \mathbf{I}(SNR_n > Th_{good})}{N}\frac{V_L}{\sum_{l=1}^{L} V_l}.\end{aligned} \tag{7}$$

The symbol powers of individual SVC layers are defined as $P_{x,l} = E[|x_{l,a}|^2] = P_{x,k} = E[|x_{k,a}|^2]$, with $l \ne k$ (where $E[\cdot]$ is the expected function and both l and k are layer indices), and should meet the transmission power at the eNB of each slot $P_{b,i} = \sum_{l=1}^{i} \sqrt{\rho_{l,i}} P_{x,l}$. In this case, the maximum value of l is i, which means that there is a total of i SVC layers that are superposed together in the i^{th} transmission slot. In the i^{th} transmission slot, the l^{th} SVC layer signal is transmitted with the power-dividing factor $\rho_{l,i}$, which is used to adjust the layer data rate or UEP in the corresponding superposed signal.

3.2.2. DNC at RS

Fig. 3 represents RS's architecture. In the second phase at the RS, in

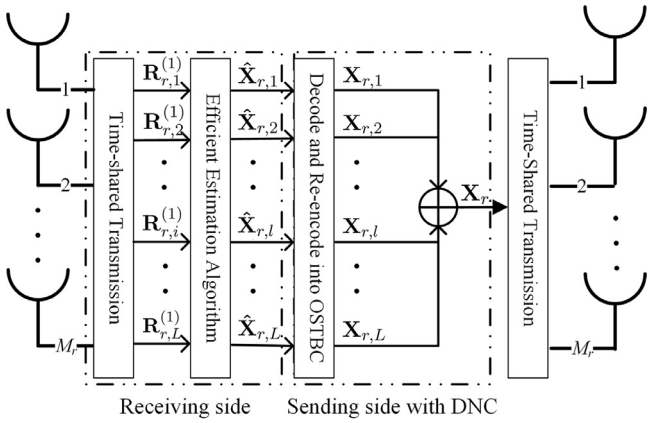

Fig. 3. Relay's architecture with the proposed EEA and DNC.

order to cancel the inter-layered interference caused from superposition coding after receiving L superposed signals from eNB in the first phase, the RS first decodes all L transmitted signals received from the eNB using the EEA (the part of receiving side in Fig. 3). We present the operation of the EEA algorithm (Algorithm 2) in the following paragraph. After using the EEA to decode all L transmitted signals, the decoded signal of each l^{th} SVC layer is then encoded into another OSTBC $\mathbf{X}_{r,\,l}$, which is used to perform DNC.

Algorithm 2 presents the proposed EEA. Note that there are L received signals in the first phase. Since the i^{th} received signal carries mainly the information of the i^{th} SVC layer, we use the terms $\mathbf{R}_{r,l}^{(1)}$ and $\mathbf{R}_{r,i}^{(1)}$, which are interchangeable. The estimation process starts from the BL through the L^{th} layer at line 2 (i.e., $(L-1)^{th}$ EL). Since the information concerning each SVC layer l exists in $L-l+1$ received signals, that is, $\mathbf{R}_{r,l}^{(1)}$ through $\mathbf{R}_{r,L}^{(1)}$, interference cancellation is performed by subtraction using the prior estimated layers first (i.e., line 3). The j^{th} subtracted signal $\widetilde{\mathbf{R}}_j^{(1)}$ of the l^{th} received signal from $\mathbf{R}_{r,l}^{(1)}$ through $\mathbf{R}_{r,L}^{(1)}$ after completely estimating $l-1$ prior SVC layer signals at line 4 is derived as follows:

$$\widetilde{\mathbf{R}}_j^{(1)} = \begin{cases} \mathbf{H}_{r,j}\sqrt{\rho_{l,j}}\mathbf{X}_l + \mathbf{N}_{r,j}^{(1)} & \text{if } j = l \\ \mathbf{H}_{r,j}\left(\sqrt{\rho_{l,j}}\mathbf{X}_l + \sum_{k=l+1}^{j}\sqrt{\rho_{k,j}}\mathbf{X}_k\right) + \mathbf{N}_{r,j}^{(1)} & \text{if } j > l \end{cases}, \tag{8}$$

where $j = [l\colon L]$ denotes the useful information superposed from $L-l+1$ received signals. At line 5, the standard decoding principles [28] treat $\mathbf{H}_{r,j}\sum_{k=l+1}^{j}\sqrt{\rho_{k,j}}\mathbf{X}_k$ as noise to estimate $\widetilde{\mathbf{X}}_j$ from $\widetilde{\mathbf{R}}_j^{(1)}$ of (8) in case of $j > l$. Otherwise, $\widetilde{\mathbf{X}}_j$ is simply estimated as in the first case in (4) for the case of $j = l$. Upon receiving all estimates from the transmitted signals of the l^{th} SVC layer, we formulate the final estimate $\widehat{\mathbf{X}}_l$ in the first phase using maximum ratio combining (MRC) [29] at line 6. Finally, the estimated signal $\widehat{\mathbf{X}}_l$ of the l^{th} SVC layer is entered into set $\mathcal{S}$ at line 7, which is used for interference cancellation in the following layer signal.

Upon obtaining all estimated SVC layer signals, the RS performs DNC to generate the network-coded signal for broadcasting in the second phase (the part of sending side with DNC in Fig. 3). Compared to conventional cooperative communication, the RS only relays one signal in the second phase in our proposed scheme instead of sequentially relaying L signals. Hence, the bandwidth efficiency can be increased. The signal matrix $\mathbf{X}_r$ transmitted by M_r antennas at the RS for a T_2 symbol duration is a linear combination of all OSTBC signals from L layers with coefficient 1 (i.e., Galois Field of 2). The received signal at UE_n is as follows:

$$\mathbf{R}_n^{(2)} = \mathbf{G}_n\mathbf{X}_r + \mathbf{N}_n^{(2)} = \mathbf{G}_n\sum_{l=1}^{L}\mathbf{X}_{r,l} + \mathbf{N}_n^{(2)}, \tag{9}$$

Input: All received signals in the first phase
Output: The set $\mathcal{S}$ of estimates of all received signals
initialization
$\mathcal{S} = \emptyset$
1: **procedure**
2: **for** l = 1 to L **do**
3: **for** j = 1 to L **do**
4: Determine the subtracted $\widetilde{\mathbf{R}}_j^{(1)}$ using the estimated signals in set $\mathcal{S}$ as input
5: Get the estimate $\widetilde{\mathbf{X}}_j$ by using the standard decoding principles from $\widetilde{\mathbf{R}}_j^{(1)}$
6: Compute the estimate of the l^{th} layer $\widehat{\mathbf{X}}_l = \sum_{j=l}^{L}\sqrt{\rho_{l,j}}P_{x,j}\widetilde{\mathbf{X}}_j$
7: $\mathcal{S} = \mathcal{S} \cup \widehat{\mathbf{X}}_l$

Algorithm 2. EEA.

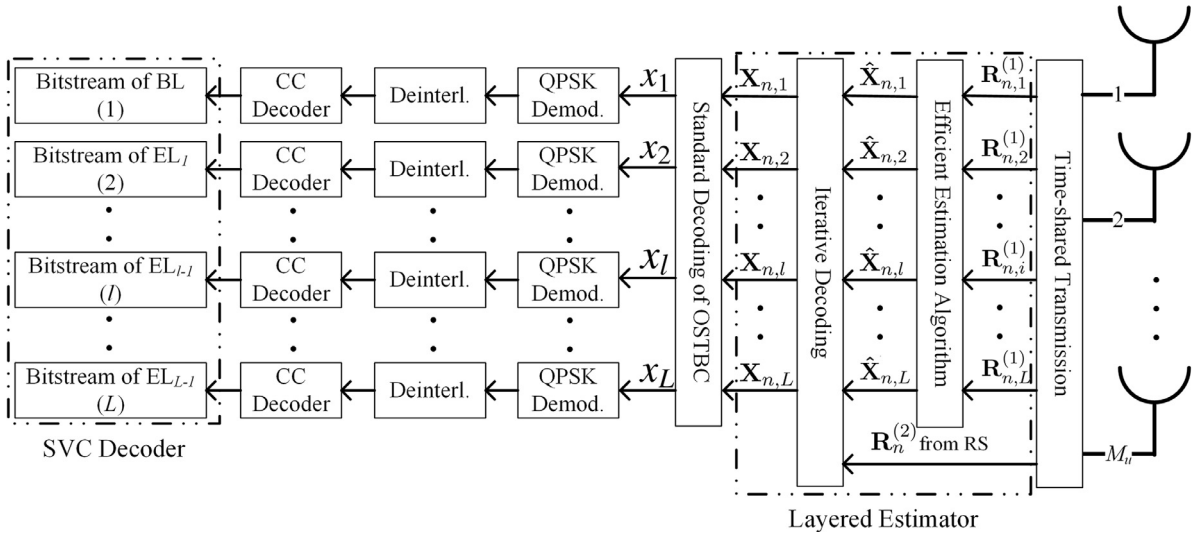

Fig. 4. UE's architecture with the proposed EEA and the iterative decoding algorithm.

where $\mathbf{N}_n^{(2)}$ is a $\mathscr{CN}(0, 1)$ distributed white noise matrix at UE$_n$ with dimensions $M_u \times T_2$. The symbol powers of individual layers at the RS are defined as $P_{r,l} = E[|x_{r,l,a}|^2] = P_{r,k} = E[|x_{r,k,a}|^2]$, with $l \neq k$ (where $x_{r,\,l,\,a}$ denotes the symbol element of the l^{th} layer at the a^{th} antenna ($a \leq M_r$ in this case) in the OSTBC of $\mathbf{X}_{r,\,l}$). They should meet $P_r = \sum_{l=1}^{L} P_{r,l}$.

3.2.3. Decoding at UE

Fig. 4 shows the process of decoding the final SVC streams at the receiver. Each UE$_n$ uses L received signals from the eNB and one network-coded signal from the RS for decoding. Thus, the two phases of the transmission are completed. The receiver uses L estimates $\widehat{\mathbf{X}}_l = \{\widehat{\mathbf{X}}_l | l = [1{:}\,L]\}$ from Algorithm 2 (i.e., EEA algorithm) in the first phase and one received signal $\mathbf{R}_n^{(2)}$ from the RS in the second phase to enhance the decoding capability by solving the inter-layer interference. We propose an IDA to decode the information of all SVC layers. The iterative decoding process of the l^{th} SVC layer is as follows:

(i) First, UE$_n$ forms the estimates of all L signals from the eNB using Algorithm 2 (i.e., EEA). Let the estimate matrix of each SVC layer be $\widehat{\mathbf{X}}_{n,l}$.

(ii) Then, using the received signal $\mathbf{R}_n^{(2)}$ from the RS and performing interference cancellation based on the information from all estimated matrices, we subtract terms with $\widehat{\mathbf{X}}_{n,k}$ in the $\mathbf{R}_n^{(2)}$ of (9), where $k = [1{:}\,L]$ and $k \neq l$, which results in a new signal:

$$\widehat{\mathbf{R}}_{n,l}^{(2)} = \mathbf{G}_n \mathbf{X}_{r,l} + \mathbf{N}_n^{(2)}, \tag{10}$$

(iii) From this subtraction, UE$_n$ can form an estimate matrix $\widetilde{\mathbf{X}}_{n,l}$ from $\widetilde{\mathbf{R}}_{n,l}^{(2)}$ using maximum-likelihood estimation [28]. Note that $\widehat{\mathbf{X}}_{n,l}$ and $\widetilde{\mathbf{X}}_{n,l}$ are the estimates of the l^{th} SVC layer signal from both eNB and RS in the two phases, respectively. Finally, we form the MRC [29] of these two estimates as $\check{\mathbf{X}}_{n,l} = \sqrt{P_{b,l}}\widehat{\mathbf{X}}_{n,l} + \sqrt{P_{r,l}}\widetilde{\mathbf{X}}_{n,l}$ to make the final decision $\mathbf{X}_{n,\,l}$ regarding decoding the transmitted signal of the l^{th} SVC layer.

We start decoding from the most important SVC layer (i.e., BL) to the $(L-1)^{th}$ layer. Upon decoding $L-1$ SVC layers, the UE simply decodes the last SVC layer (i.e., the least important SVC layer) by using the decoded information from $L-1$ prior SVC layers. Hence, the diversity order can be achieved by two signals (one from eNB and another from RS) at the cost of decoding complexity. Moreover, alternative layers yield better performance in terms of data rate.

4. Capacity analysis of scalable video multicast

In this section, we use channel capacity (bps/Hz) to evaluate the performance of the proposed schemes. Channel capacity refers to an information rate that the receiver can achieve except the error-correcting code. It is easily achieved with negligible error rate by using modern channel codes such as low-density parity check, turbo, and Raptor. Hence, capacity analysis is widely used to evaluate the transmission performance of modern channel-coded wireless systems.

Let $I_{gain,\,l}$ be the information gain of the l^{th} SVC layer, except the L^{th} layer. Information from a lower layer is hierarchically superposed into the transmission of a higher layer. After applying the interference cancellation technique to each layer, all signals that are superposed in the same transmission that cannot be used in decoding are treated as interference. The information gain of the l^{th} SVC layer can be defined as follows:

$$I_{gain,l} = \sum_{j=l+1}^{L} \frac{\rho_{l,j} \, \|\mathbf{H}_{n,j}\|^2 P_{x,j}}{\sum_{k=l+1}^{j} \rho_{k,j} \, \|\mathbf{H}_{n,j}\|^2 P_{x,k} + 1}, \tag{11}$$

where j is the index of the transmission slot and k is the SVC layer index of the superposed signal.

The channel capacity [7] of the l^{th} SVC layer, except the L^{th} layer, at UE$_n$ after receiving L signals from the eNB in the first phase is as follows:

$$C_l^{(1)} = \frac{1}{2} r_s \log\left(1 + \rho_{l,l} \, \|\mathbf{H}_{n,l}\|^2 \frac{P_{x,l}}{M_b} + I_{gain,l}\right), \tag{12}$$

where subscript l represents the layer index, superscript (1) indicates a transmission phase of 1, $\frac{1}{2}$ means that the eNB operates in the half-duplex mode, and r_s is the spatial code rate, which is the ratio of the number of independent data symbols to the transmission duration of OSTBC. The spatial rate decreases as the number of transmitting antennas increases due to OSTBC (i.e., $r_s < 1$). The relevant channel capacity $C_{r,\,l}$ at the RS is similar to that given in Eq. (12) with the replacement of the channel state matrix from $\mathbf{H}_{n,\,l}$ to $\mathbf{H}_{r,\,l}$.

Finally, the channel capacity of the l^{th} SVC layer after the complete transmission is given by the following expression, with additional information gain received from the RS in the second phase:

$$C_l = \frac{1}{2} r_s \log\left(1 + \rho_{l,l} \, \|\mathbf{H}_{n,l}\|^2 \frac{P_{x,l}}{M_b} + I_{gain,l} + \left\|\mathbf{G}_n\right\|^2 \frac{P_{r,l}}{M_r}\right). \tag{13}$$

According to the last EL, there is no more interference following subtraction by using $L-1$ prior estimates. Hence, the relevant channel

Table 1
Simulation parameters.

Parameter	Value
System bandwidth	320 KHz
Carrier frequency	2.0 GHz
Transmission power at eNB	46 dBm
Transmission power at RS	26 dBm
Antenna gains	eNB: 14 dBi, UE: 0 dBi
Antenna height	eNB: 60 m, RS: 30 m, UE: 1.5 m
Penetration loss	20 dB
Radio frequency propagation model	Okumura-Hata model
Shadowing	Standard deviation: 7 dB
Noise figure	7 dB
H.264/SVC video stream	Soccer CIF with $L = 3$
Channel state threshold (dB)	Th_{fair}: 5; Th_{good}: 10
Target video bitrate (Kbps)	V_1: 640; V_2: 320; V_3: 192
GOP	16 frames
Frame rate	30 fps

capacity can be presented as follows:

$$C_L = \frac{1}{2} r_s \log\left(1 + \rho_{L,L} \|\mathbf{H}_{n,L}\|^2 \frac{P_{x,L}}{M_b} + \left\|\mathbf{G}_n\right\|^2 \frac{P_{r,L}}{M_r}\right). \quad (14)$$

As seen above, the proposed multicast transmission scheme not only reduces the number of additional transmissions to one but also guarantees performance gain from cooperation with UEP for a scalable video.

5. Performance evaluation

In this section, we present the evaluation of the performance of the proposed video multicast method from three viewpoints: relevant capacity, achievable video bitrate, and PSNR. Each simulation was run 100,000 times with a confidence interval of at least 95% in the Matlab environment. We performed numerical simulations with an antenna configuration of $M_b = 4$, $M_r = 4$, and $M_u = 2$, a channel medium of the Rayleigh channel, and a spatial code rate r_s of $\frac{3}{4}$. To avoid the peak-to-average power ratio [30] due to superposition coding, we maintained the same transmission power for all layers (i.e., $P_b = P_{b,i} = P_{b,j}$ with $i \neq j$; note that i and j are indices of transmission slot) in the first phase. Table 1 describes the main simulation parameters. The video content was partitioned into three scalable video layers consisting of one BL and two ELs. The target video bitrates of *BL*, EL_1, and EL_2 SVC layers were 640, 320, and 192 Kbps, respectively, corresponding to the various video qualities of 432, 360, and 240 p [31] (where p stands for "progressive" and 240 p means that all 240 lines are drawn in each frame). If the UE receives only the BL, the desired video quality is 240 p, both BL and EL_1 correspond to 360 p, and so on.

First, we performed simulation with three fixed IDF sets to evaluate the capability of providing UEP among SVC layers in terms of relevant capacity and achievable video bitrate.

- IDF set 1 (i.e., good channel state): using Eq. (5) according to the good channel state, hence IDF set 1 ($\beta_1 = 0.5556$, $\beta_2 = 0.2778$, $\beta_3 = 0.1667$).
- IDF set 2 (i.e., fair channel state): assume that the 30% power resource of EL_2 is moved to assign for BL additionally, hence IDF set 2 ($\beta_1 = 0.6056$, $\beta_2 = 0.2778$, $\beta_3 = 0.1167$).
- IDF set 3 (i.e., bad channel state): the 30% and 70% power resources of EL_1 and EL_2, respectively, are moved to assign for BL, hence IDF set 3 ($\beta_1 = 0.7556$, $\beta_2 = 0.1945$, $\beta_3 = 0.0500$).

Second, for comparison of video quality measurement with other multicast schemes, we evaluated the PSNR performance of the received SVC streams with various settings in terms of RS's transmission range (i.e., RS's coverage) and network size (i.e., the number of UEs in a multicast group). Note that the IDF set is adaptively determined at each transmission duration of L SVC layers according to the channel states of UEs.

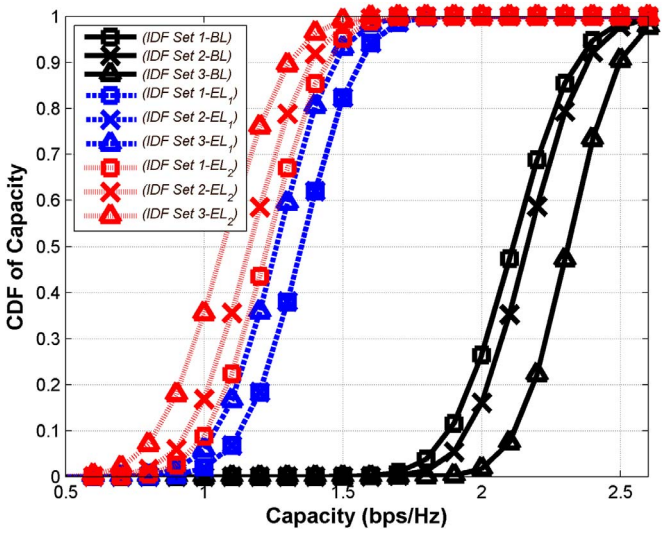

Fig. 5. CDF curves of layer capacities in various IDF sets.

5.1. Outage events and data rates of scalable layers

To specify scalability with ISC, suppose that the total capacity of the original video signal at the video encoder is R_0 bps/Hz. This is divided into multiple rates R_l bps/Hz, with a base rate of R_1 bps/Hz, and several enhancement rates ranging from R_2 to R_L bps/Hz; the total rate is $R_0 \geq \sum_{l=1}^{L} R_l$ in general. We define that the outage event at UE, O_l, is the outage event of the l^{th} SVC layer at UE_n, where $C_l \leq R_l$ with $\overline{O}_l$. The video rate of each l^{th} SVC layer can be achieved by the allocation of IDF β_l, such that the O_l outage is less than a certain probability with UE_n near the edge of the macrocell area, in order to guarantee system performance in a video multicast scheme with channel heterogeneity. The target acceptable error probability is generally 10% [32].

Fig. 5 shows the cumulative density functions (CDFs) of C_1, C_2, and C_3 with three settings of the IDFs: set 1, set 2, and set 3 predefined in Section 5. According to these curves, we can choose the probability $P(O_l)$ of the corresponding l^{th} SVC layer outage event. For instance, we can keep $P(O_l) \leq 0.1$ for all SVC layers depending on the selection of the IDFs, and the rates can be achieved according to the corresponding IDF set:

- IDF set 1 ($\beta_1 = 0.5556$, $\beta_2 = 0.2778$, $\beta_3 = 0.1667$): $R_1 \leq 1.82$ bps/Hz, $R_2 \leq 1.15$ bps/Hz, and $R_3 \leq 1$ bps/Hz (the lines with square markers).
- IDF set 2 ($\beta_1 = 0.6056$, $\beta_2 = 0.2778$, $\beta_3 = 0.1167$): $R_1 \leq 1.9$ bps/Hz, $R_2 \leq 1.15$ bps/Hz, and $R_3 \leq 0.9$ bps/Hz (the lines with cross markers). As seen, R_1 increases with the cost of R_3.
- IDF set 3 ($\beta_1 = 0.7556$, $\beta_2 = 0.1945$, $\beta_3 = 0.0500$): $R_1 \leq 2.15$ bps/Hz, $R_2 \leq 1.05$ bps/Hz, and $R_3 \leq 0.76$ bps/Hz (the lines with triangle markers).

The results showed that the proposed inter-layered superposition can provide UEP, and satisfactorily matches the specific characteristic of the scalable video, where the capacity of the BL yielded the highest performance, followed by the subsequent ELs. The allocation of IDFs adjusted the data rates of layers matching the changeable ability of the given target video bitrate. The outage probability of each SVC layer was negligible due to a sufficiently strong link channel medium between the eNB and RS (i.e., various transmission powers), as well as sufficiently small data rates for all layers corresponding to the given rates.

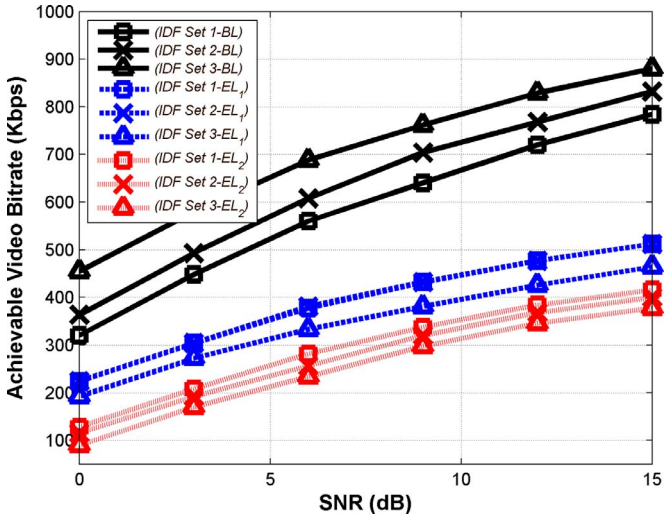

Fig. 6. Achievable video bitrates of scalable layers.

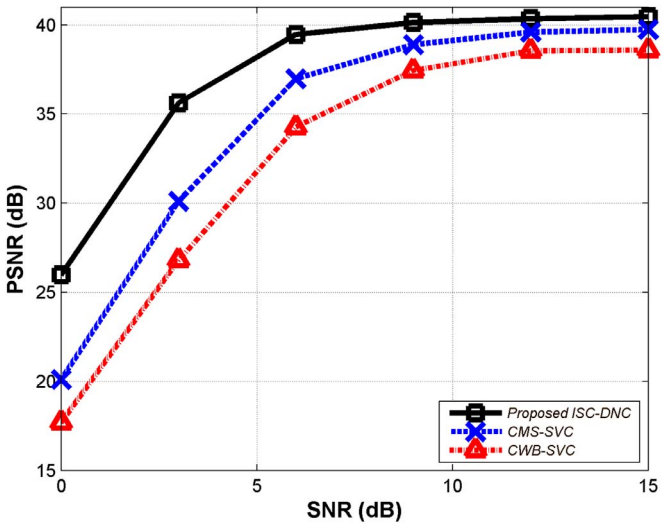

Fig. 7. PSNR versus SNR with respect to UE.

5.2. Achievable video bitrate performance

Based on the basic analysis and numerical results from Sections 4 and 5.1, we derived the corresponding achievable video bitrates of the scalable video layers shown in Fig. 6. The transmission bandwidth included two resource blocks of 180 kHz, which followed the spectrum allocation from the IMT-Advanced guidelines for the long-term evolution (LTE) standard [26].

Fig. 6 shows the achievable video bitrates of all scalable layers corresponding to various IDFs of sets 1–3 under the given different target video bitrates and outage probability constraints (i.e., 10%), respectively. Note that each IDF set represents a channel state classified in Section 3.1. The simulation results satisfactorily matched our design objective. The achievable video rates of all SVC layers were various rates with the highest bitrate of BL followed by ELs. As the channel state was good, the achievable video rates of all three SVC layers matched the target video bitrates. As the channel state was fair, only BL and EL_1 layers satisfied the target video bitrates. Consequently, as the channel state was bad, only one BL layer could satisfy the target video bitrate. Hence, our ISC-DNC could classify the multicast group into three subgroups (i.e., good, fair, or bad UEs), experiencing different perceptual video quality performance. When many UEs experienced poor channel conditions, the SNR was not strong enough for the UEs to decode all SVC layers. In this case, the IDF set 3 could enhance a greater number of UEs decoding the BL. A typical video quality was achieved because more UEs could render the BL under a bad channel condition. Hence, the proposed scheme could provide the UEs with UEP and scalability. Our proposed ISC-DNC scheme provided a flexible allocation of importance among SVC layers by controlling the IDF parameters corresponding to the target video bitrates.

5.3. Comparison of video quality measurements

For a comparison of video quality measurements, we used the JSVM 9.19 reference software [33] to encode scalable video bitstreams into multiple layers with SNR scalability. PSNR was selected as a video performance metric with the transmission of the *Soccer* sequence, which consisted of 150 frames, CIF resolution of 352 x 288 pixels, and a group-of-picture size of 16 frames with a hierarchical B-picture prediction (HBP) structure. The HBP structure is a typical coding method in SVC that can support quality scalability with high coding efficiency. Two cooperative schemes with superposition coding for scalable video transmission (i.e., CWB-SVC [6] and CMS-SVC [7]) were chosen for comparison, with an antenna configuration of $M_b = 4$, $M_r = 2$, and $M_u = 2$. The *Soccer* sequence was encoded into two layers instead of three as the transmission mode because the eNB can convey a maximum of two layers in their schemes.

We performed the video measurement with two scenarios: unicast and multicast. Fig. 7 represents the PSNR performance versus SNR performance with respect to a UE. ISC-DNC achieved the best performance in comparison with CMS-SVC and CWB-SVC. As a worse channel condition, the performance gain could obtain greater achievement since more UEs could decode the BL. The results demonstrated that ISC-DNC showed better performance as the channel state worsened. As the channel condition became better, the performance of the three schemes became closer to each other.

For a multicast scenario, we performed simulation with a multicast group of 50 UEs, which were distributed uniformly in the RS's coverage (i.e., transmission range). We evaluated the video performance with various RS transmission ranges. As the transmission range increases, it means that there are more UEs experiencing a bad channel state; the mean value of SNR also decreases. Our proposed ISC-DNC outperformed CMS-SVC and CWB-SVC in terms of video quality measurement in the multicast scenario shown in Fig. 8. The results showed that ISC-DNC achieved a better performance gain as the transmission range

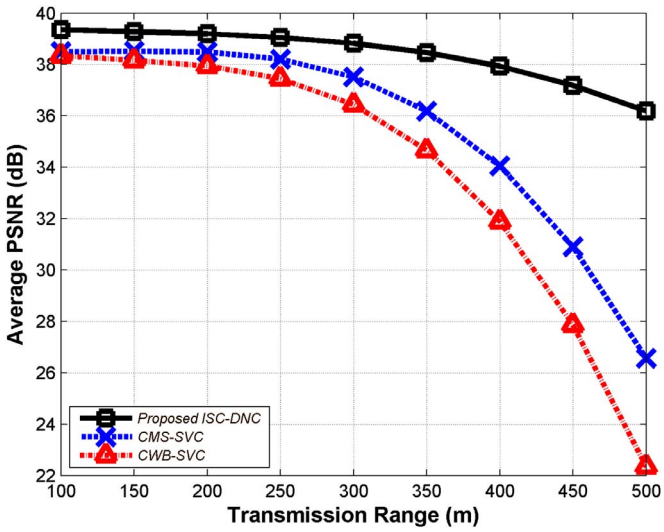

Fig. 8. Average PSNR versus RS's transmission range with the multicast group of 50 UEs.

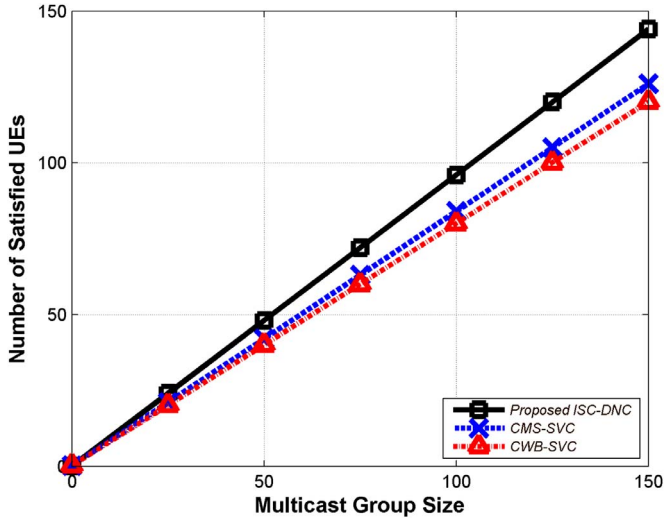

Fig. 9. Number of satisfied UEs versus the multicast group size (i.e., network size and number of UEs were distributed within RS's transmission range of 300 m).

increased. This was because ISC-DNC could increase the importance of the BL by adaptively adjusting the IDF set. To evaluate the effectiveness of IDF adaptation, we defined the number of satisfied UEs, which is the number of UEs enabling to render the BL shown in Fig. 9. We conducted performance evaluation with diverse multicast groups. As seen, the number of satisfied UEs increased with the group size. The results demonstrated that IDF adaptation can provide efficient protection for the BL.

6. Conclusion

Herein, we proposed a practical scalable video multicast scheme according to channel conditions at the time of transmission over dedicated relay-based cellular networks. We performed a capacity analysis on the achievable video bitrate performance and a comparison with prevalent methods in terms of video quality measurements. The proposed ISC-DNC is applicable to scalable video multicast with simple operational control of IDF parameters. Depending on the target video bitrate and channel conditions, the operation of suitable IDF control was flexibly performed with outage less than a certain probability so that the system performance could be guaranteed to be satisfactory. The proposed combination of ISC with an EEA and network-coded cooperation provided UEP and bandwidth efficiency under channel heterogeneity. In particular, ISC-DNC could increase the number of UEs experiencing fully supported video quality. The UEP characteristic of the scalable video was handled by the proposed inter-layered superposition with the EEA, while the issue of additional transmission resources for cooperative communication was tackled by performing DNC at a dedicated relay. Only one more transmission at the relay for cooperation was required for spatial diversity and bandwidth efficiency. Recently, the need for expanding the coverage and system capacity has been increasing, and research on multiple relays is also being considered. As future work, we will extend our scheme to cover cases involving multiple relays and high mobility of UEs.

Acknowledgments

This work was supported by Institute for Information & communications Technology Promotion (IITP) grant funded by the Korea government (MSIT) (No. 2013-3-00409, Research and Development of 5G Mobile Communications Technologies using CCN-based Multi-dimensional Scalability).

References

[1] H. Bobarshad, M. van der Schaar, M.R. Shikh-Bahaei, A low-complexity analytical modeling for cross-layer adaptive error protection in video over Wlan, IEEE Trans. Multimedia 12 (5) (2010) 427–438.
[2] F. Babich, M. Comisso, R. Corrado, F. Merazka, Joint voice/video retry limit adaptation for on-demand streaming over wifi networks, IEEE Commun. Letters 20 (9) (2016) 1852–1855.
[3] O. Alay, P. Liu, Y. Wang, E. Erkip, Cooperative layered video multicast using randomized distributed space time codes, IEEE Trans. Multimedia 13 (5) (2011) 1127–1140.
[4] S.P. Chuah, Z. Chen, Y.P. Tan, Energy-efficient resource allocation and scheduling for multicast of scalable video over wireless networks, IEEE Trans. Multimedia 14 (4) (2012) 1324–1336.
[5] S.C. Wang, W. Liao, Cooperative multicasting for wireless scalable video transmissions, IEEE Trans. Commun. 61 (9) (2013) 3980–3989.
[6] C.H. Kuo, C.M. Wang, J.L. Lin, Cooperative wireless broadcast for scalable video coding, IEEE Trans. on Circuits and Sys. Video Tech. 21 (6) (2011) 816–824.
[7] D. Hwang, P. Chau, J. Shin, T.J. Lee, Two cooperative multicast schemes of scalable video in relay-based cellular networks, IET Commun. 9 (7) (2015) 982–989.
[8] P. Chau, Y. Lee, J. Shin, A comparison of transmission schemes for scalable video over mimo relay networks, ICACT (2014) 234–238.
[9] Z. Yang, X. Wang, Scalable video broadcast over downlink mimo-ofdm systems, IEEE Trans. on Circuits and Sys. Video Tech. 23 (2) (2013) 212–223.
[10] H. Schwarz, D. Marpe, T. Wiegand, Overview of the scalable video coding extension of h.264/AVC, IEEE Trans. Circuits and Sys. Video Tech. 17 (9) (2007) 1103–1120.
[11] Y. Zhang, Z. Ni, C.H. Foh, J. Cai, Retry limit based ulp for scalable video transmission over ieee 802.11e wlans, IEEE Commun. Letters 11 (6) (2007) 498–500.
[12] Cisco visual networking index: global mobile data traffic forecast update, 2016–2021 White Paper:http://www.cisco.com.
[13] C. Li, J. Zhang, K.B. Letaief, Throughput and energy efficiency analysis of small cell networks with multi-antenna base stations, IEEE Trans. Wireless Commun. 13 (5) (2014) 2505–2517.
[14] X. Ge, S. Tu, G. Mao, C.X. Wang, T. Han, 5G ultra-dense cellular networks, IEEE Trans. Wireless Commun. 23 (1) (2016) 72–79.
[15] S.Y. Baek, Y.J. Hong, D.K. Sung, Adaptive transmission scheme for mixed multicast and unicast traffic in cellular systems, IEEE Trans. Vehicular Tech. 58 (6) (2009) 2899–2908.
[16] G. Feng, Y. Zhang, J. Lin, H. Wang, L. Cai, Joint optimization of downlink and d2d transmissions for SVC streaming in cooperative cellular networks, Neurocomputing 270 (2017) 178–187.
[17] A. Douik, S. Sorour, T.Y. Al-Naffouri, M.S. Alouini, Instantly decodable network coding: from centralized to device-to-device communications, IEEE Commun. Surveys Tutorials 19 (2) (2017) 1201–1224.
[18] M.S. Karim, A. Douik, S. Sorour, Rate-aware network codes for video distortion reduction in point-to-multipoint networks, IEEE Trans. Vehicular Tech. 66 (8) (2017) 7446–7460.
[19] J. Kim, J. Cho, H. Shin, Layered resource allocation for video broadcasts over wireless networks, IEEE Trans. Consumer Electronics 54 (4) (2008) 1609–1616.
[20] A. de la Fuente, J.J. Escudero-Garzás, A. García-Armada, Radio resource allocation for multicast services based on multiple video layers, IEEE Trans. Broadcasting (99) (2017) 1–14.
[21] S. Huang, E. Izquierdo, P. Hao, Adaptive packet scheduling for scalable video streaming with network coding, J. Visual Commun. Image Representation 46 (2017) 10–20.
[22] R. Ahlswede, N. Cai, S.Y.R. Li, R.W. Yeung, Network information flow, IEEE Trans. Inform. Theory 46 (4) (2000) 1204–1216.
[23] M. Peng, H. Liu, W. Wang, H.H. Chen, Cooperative network coding with mimo transmission in wireless decode-and-forward relay networks, IEEE Trans. Vehicular Tech. 59 (7) (2010) 3577–3588.
[24] S. Sharma, Y. Shi, J. Liu, Y.T. Hou, S. Kompella, S.F. Midkiff, Network coding in cooperative communications: friend or foe? IEEE Trans. Mobile Computing 11 (7) (2012) 1073–1085.
[25] P. Chau, S. Kim, Y. Lee, J. Shin, Hierarchical random linear network coding for multicast scalable video streaming, APSIPA (2014).
[26] H. Zarrinkoub, Understanding LTE with MATLAB from mathematical modeling to simulation and prototyping, John Wiley & Sons, 2014.
[27] Making sense of signal strength/signal quality readings for cellular modems: http://www.industrialnetworking.com.
[28] V. Tarokh, H. Jafarkhani, A.R. Calderbank, Space-time block codes from orthogonal designs, IEEE Trans. Inform. Theory 45 (5) (1999) 1456–1467.
[29] K.S. Ahn, R.W. Heath Jr, Performance analysis of maximum ratio combining with imperfect channel estimation in the presence of cochannel interferences, IEEE Trans. Wireless Commun. 8 (3) (2009) 1080–1085.
[30] J. Tong, L. Ping, X. Ma, Superposition coded modulation with peak-power limitation, IEEE Trans. Inform. Theory 55 (6) (2009) 2562–2576.
[31] J.R.C. Patterson, Video encoding settings for H.264 excellence: http://www.lighterra.com.
[32] A. Tassi, C. Khirallah, D. Vukobratovic, F. Chiti, J.S. Thompson, R. Fantacci, Resource allocation strategies for network-coded video broadcasting services over lte-advanced, IEEE Trans. Vehicular Tech. 64 (5) (2015) 2186–2192.
[33] SVC reference software: http://www.hhi.fraunhofer.de.